




RESEARCH ARTICLE

CSF parvalbumin levels reflect interneuron loss linked with cortical pathology in multiple sclerosis

Roberta Magliozzi^{1,2} , Marco Pitteri^{1,a} , Stefano Ziccardi^{1,a}, Anna Isabella Pisani¹, Luigi Montibeller¹, Damiano Marastoni¹, Stefania Rossi³, Valentina Mazziotti¹, Maddalena Guandalini¹, Caterina Dapor¹, Gianmarco Schiavi¹, Agnese Tamanti¹, Richard Nicholas² , Richard Reynolds^{2,a} & Massimiliano Calabrese^{1,a}

¹Neurology Section, Department of Neurosciences, Biomedicine and Movement Sciences, University of Verona, Verona, Italy

²Division of Neuroscience, Department of Brain Sciences, Imperial College London, London, United Kingdom

³Department of Oncology and Molecular Oncology, Istituto Superiore di Sanità, Rome, Italy

Correspondence

Roberta Magliozzi, Neurology Section, Department of Neurosciences, Biomedicine and Movement Sciences, University of Verona, Italy. Tel: +39-045-8126017; Fax: +39-045-8027276; E-mail: roberta.magliozzi@univr.it

Funding Information

Magliozzi and Tamanti were supported by Italian MS Foundation grant (FISM 16/17/ F14). Calabrese and Rossi were supported by the GR-2013-02-355322 grant from Italian Ministry of Health. Reynolds and Nicholas were supported by the MS Society of Great Britain and Northern Ireland (grant 910/09), the National Institute for Health Research Biomedical Research Centre at Imperial College and the EU 6th Framework Network of Excellence BrainNetEurope II.

Received: 17 June 2020; Revised: 15 October 2020; Accepted: 11 November 2020

Annals of Clinical and Translational Neurology 2021; 8(3): 534–547

doi: 10.1002/acn3.51298

^aThese authors equally contributed to this work.

Introduction

Multiple Sclerosis (MS) is the commonest inflammatory neurodegenerative disorder of the human central nervous system (CNS), characterized histologically by multifocal areas of inflammation, demyelination, and

Abstract

Introduction and methods: In order to verify whether parvalbumin (PVALB), a protein specifically expressed by GABAergic interneurons, could be a MS-specific marker of grey matter neurodegeneration, we performed neuropathology/molecular analysis of PVALB expression in motor cortex of 40 post-mortem progressive MS cases, with/without meningeal inflammation, and 10 control cases, in combination with cerebrospinal fluid (CSF) assessment. Analysis of CSF PVALB and neurofilaments (Nf-L) levels combined with physical/cognitive/3TMRI assessment was performed in 110 naïve MS patients and in 32 controls at time of diagnosis. **Results:** PVALB gene expression was downregulated in MS (fold change = 3.7 ± 1.2 , $P < 0.001$ compared to controls) reflecting the significant reduction of PVALB+ cell density in cortical lesions, to a greater extent in MS patients with high meningeal inflammation (51.8 , $P < 0.001$). Likewise, post-mortem CSF-PVALB levels were higher in MS compared to controls (fold change = 196 ± 36 , $P < 0.001$) and correlated with decreased PVALB+ cell density ($r = -0.64$, $P < 0.001$) and increased MHC-II+ microglia density ($r = 0.74$, $P < 0.01$), as well as with early age of onset ($r = -0.69$, $P < 0.05$), shorter time to wheelchair ($r = -0.49$, $P < 0.05$) and early age of death ($r = -0.65$, $P < 0.01$). Increased CSF-PVALB levels were detected in MS patients at diagnosis compared to controls ($P = 0.002$). Significant correlation was found between CSF-PVALB levels and cortical lesion number on MRI ($R = 0.28$, $P = 0.006$) and global cortical thickness ($R = -0.46$, $P < 0.001$), better than Nf-L levels. CSF-PVALB levels increased in MS patients with severe cognitive impairment (mean \pm SEM: 25.2 ± 7.5 ng/mL) compared to both cognitively normal (10.9 ± 2.4 , $P = 0.049$) and mild cognitive impaired (10.1 ± 2.9 , $P = 0.024$) patients. **Conclusions:** CSF-PVALB levels reflect loss of cortical interneurons in MS patients with more severe disease course and might represent an early, new MS-specific biomarker of cortical neurodegeneration, atrophy, and cognitive decline.

neurodegeneration^{1,2} within the white matter³ (WM), but also within cortical and deep grey matter⁴ (GM). GM pathology is present in the MS brain since the earliest stages of the disease^{5,6} and accumulates, in particular, in the progressive phase,^{7,8} contributing to the increase in physical disability^{9,10} and cognitive impairment.^{11,12}

Brain-imaging studies have confirmed that cortical thinning occurs prominently in areas of the brain that have extensive cortico-cortico connections, such as the cingulate gyrus, insula and superior frontal gyrus, while, primary sensory and visual areas are less significantly involved.¹³ A “surface-in” gradient of neuronal loss has been identified in the motor cortex of post-mortem MS cases with elevated meningeal inflammation characterized by the presence of lymphoid-like structures and a more aggressive disease course.^{14,15} Cortical neuronal vulnerability and damage in the upper cortical layers, including both dysfunction and loss, is now thought to be a major contributor to the progression of MS,^{16–18} independently from cortical demyelination. However, following the progression of neurodegeneration *in vivo* has so far proven elusive.

Recent evidence has confirmed an association between CSF inflammatory protein profile, meningeal inflammation and GM damage, as visualized with advanced MRI techniques.^{19,20} In addition, proinflammatory cytokines/chemokines together with neurofilament proteins are suggested to be useful biomarkers of cortical pathology and neurodegeneration in MS.²⁰ Neurofilament light chain (Nf-L) is a cytoskeletal component of neurons, particularly abundant in axons, that is released into the extracellular space following axonal destruction and then drains into the CSF, thus providing an indication of axonal damage and neuronal death. Nf-L levels are increased in the CSF of MS patients who convert earlier to secondary progression.²¹ However, increased CSF levels of Nf-L occur in all neurodegenerative conditions, including stroke,²² amyotrophic lateral sclerosis,²³ and frontotemporal dementia.²⁴ We recently reported a substantial reduction in PVALB gene expression in both demyelinated and nondemyelinated regions of the motor cortex of post-mortem secondary progressive MS (SPMS) brains, which reflected the degree of meningeal inflammation and cortical neurodegeneration, whereas the reduction in expression of the Nf-L gene did not reflect these pathologies.²⁵ This suggests that changes in PVALB protein levels in the CSF might give a more accurate and specific indication of the degree of ongoing cortical neurodegeneration than Nf-L.

PVALB is a calcium binding protein expressed in a subset of GABA-ergic inhibitory cortical interneurons and PVALB expressing cells have been classified as fast-spiking interneurons.²⁶ PVALB is known to buffer calcium ion levels and has been shown to protect neurons from excess intracellular calcium.^{27,28} Previous observations in MS showed a decrease in GABA-ergic PVALB⁺ interneurons in layer II of the primary motor cortex of MS patients, in particular within the NAGM.^{29,30} Furthermore, a significant correlation between numbers of PVALB expressing

cells and age at death was found, suggesting a possible association between MS disease duration and loss of PVALB interneurons.³⁰ Our previous data showing decreased PVALB gene expression in MS cases with a more rapid and severe disease progression and increased cortical pathology²⁵ suggests the possibility of using PVALB protein levels as a biomarker for cortical GM neurodegeneration to identify at an early stage those individuals at risk of a more severe and rapid MS disease progression.

In the present study, we investigated the extent of PVALB⁺ cell loss in cortical lesions in the motor cortex of post-mortem MS cases compared to control cases and measured PVALB protein levels in paired CSF samples. Moreover, we conducted a combined *in-vivo* CSF and 3T-MRI analysis, together with clinical and neuropsychological assessments, in a cohort of MS patients at the time of diagnosis, in order to evaluate if PVALB may represent a specific biomarker associated with cortical neurodegeneration, demyelination, and atrophy even in the earliest disease stages.

Materials and Methods

Neuropathological study

Post-mortem MS and control tissues

All post-mortem tissues were obtained from the UK MS Society Tissue Bank at Imperial College London (London, UK) and were obtained at autopsy with fully informed consent under ethical approval by the National Research Ethics Committee (08/MRE09/31), with the exception of three controls provided by University of Verona (Verona, Italy). Demographic/clinical/ neuropathological characteristics of the SPMS cases and controls are shown in Table 1. The clinical diagnosis of SPMS (median post-mortem delay = 14.4 h) was confirmed based on the patient medical history and a detailed neuropathological analysis as described previously.¹ The neuropathological study was performed on two independent groups of post-mortem SPMS cases: (1) precentral gyrus snap frozen tissue blocks from a cohort of 20 post-mortem cases of SPMS previously characterized for the presence ($n = 10$, FposSPMS) or absence ($n = 10$, FnegSPMS) of tertiary lymphoid-like tissues in the leptomeninges¹⁴; (2) precentral gyrus paraffin tissue blocks from an independent cohort of 20 post-mortem cases of SPMS previously characterized for the presence of elevated (10 MShigh) or low (10 MSlow) levels of meningeal inflammation.²⁰ In addition, 13 non-neurological control cases (median post-mortem delay = 12 h; median age at death = 58 years) have been also analyzed.

Table 1. Clinical and demographic details of examined post-mortem MS cases.

MS case	Sex	Age of onset (years)	Age wheelchair (years)	Disease duration (years)	Age at death (years)
I Group					
Fneg MS					
3	M	34	46	21	55
42	M	29	46	22	51
56	M	24	39	39	63
74	F	28	50	36	64
100	M	37	38	9	46
104	M	41	46	12	53
114	F	37	39	15	52
127	M	28	44	24	52
163	F	39	41	6	45
200	M	19	28	24	43
Fpos MS					
MS79	F	25	35	24	49
MS92	F	20	28	18	38
121*	F	35	36	35	35
124	F	24	26	24	24
180*	F	25	26	25	25
197*	F	24	46	27	51
230*	F	22	35	22	22
234*	F	24	31	15	39
256*	F	29	38	24	53
286*	M	29	34	29	29
II Group					
MS-Low					
296	M	19	48	40	59
301	F	21	36	41	62
304	M	29	37	23	52
318	F	25	46	34	59
347	M	22	47	28	50
364	F	22	32	34	56
422	M	No data	No data	58	58
444	M	28	31	21	49
461	M	23	32	20	43
485	F	27	50	57	57
MS-High					
407	F	25	33	19	44
MS402	M	25	37	21	46
MS408	M	28	36	11	39
MS423	F	24	33	30	54
MS438	F	17	49	36	53
MS473	F	9	32	31	40
MS497	F	45	47	15	60
MS510	F	16	23	22	38
MS513	M	33	40	18	51
MS527	M	21	33	25	46

Gene expression analysis

Gene ontology (GO) analyses were performed using DAVID Bioinformatics resources (6.8) on Illumina whole genome HumanRef8 v2 BeadChip expression array data, from grey matter tissue dissected from the precentral

gyrus snap frozen tissue blocks, that was previously described and reported.²⁵ Protein-protein interaction (PPI) analysis was performed by using STRING software (version 11.0) and Cytoscape software (version 3.7.1) was used to visualize the PPI analysis.

Immunohistochemistry and analysis

Quantitative analysis of the distribution and density of PVALB+ neurons was performed by counting PVALB+ cells on both sections cut from the snap frozen precentral gyrus blocks of the first cohort and on sections of formalin fixed paraffin embedded (FFPE) precentral gyrus blocks of the second cohort, in comparison with to the respective control cases. PVALB+ cells were identified by immunohistochemical localization of PVALB protein expression using a rabbit anti-PVALB antibody (SWANT, Rte Ancienne Papeterie, Switzerland). Double immunohistochemistry with mouse anti-NeuN antibody (Chemicon International, Temecula, CA) was performed in order to confirm the expression of PVALB on neurons (Fig. 1). Briefly, snap frozen sections and dewaxed paraffin sections from precentral gyrus were dehydrated and immunostained with myelin oligodendrocyte (MOG), major histocompatibility class II (MHC class-II) and PVALB detecting antibodies following the immunohistochemistry procedures previously described^{15,31}. Antibody binding was visualized using peroxidase or alkaline phosphatase systems (Vector Labs, Peterborough, UK) and images were acquired with Axiophot (ZEISS) microscope. For each case of the two MS cohorts and of control group, four random fields (20× objective) were acquired in type III cortical lesions and NAGM, by considering a central rectangular grid (0.032 mm²) drawn in each acquired field to avoid the simultaneous analysis of adjacent layers. Results were expressed as cell density/mm². The 4 adjacent fields were acquired from the pial surface toward the WM, covering all the 6 cortical grey matter layers in order to assess the density of all the PVALB+ neurons and to avoid any bias due to the layer to layer variation. The counts were performed blinded (RM) with respect to the disease/control condition on three consecutive sections immunostained with PVALB antibody for each examined case and the means and standard errors were calculated. Both manual and automatic (QuPath Analysis) methods were tested and were almost completely comparable, but the manual count was finally selected as it helped exclude any nonspecific objects.

CSF post-mortem analysis

The PVALB levels were measured in duplicate in the available CSF samples available from the second MS

group (Table 1) using a Human Parvalbumin ELISA kit (MBS2022353, MyBioSource, San Diego, CA, USA) according to the manufacturer's instructions. Briefly, the precoated wells were incubated with 100 μ L of a 1:1 dilution of the post-mortem CSF for 2 h at 37°C and then incubated with reagent A for 1 h at 37°C. After washing the samples were incubated with reagent B at 37°C for 30 min and incubated with TBM ELISA substrate at 37°C after washing. The reaction was stopped after 20 min with a specific solution and the optical density was measured at 450 nm on a Model 680 Series microplate reader (Bio-Rad). Samples were analyzed in random order and staff were blinded to the treatment arms. The detection threshold was of 0.55 ng/mL. Intra-assay variability (coefficients of variation) of the samples was below 10%. The levels of neurofilament protein light chain (Nf-L) in post-mortem CSF samples were measured using a Human Nf-L ELISA kit (MyBioSource, San Diego, CA, USA) according to previously optimized procedures²⁰ and the quantification was carried out on a VICTOR X3 2030 Multilabel Plate Reader (Model 680 Series microplate reader, Bio-Rad) with a detection threshold of 0.06 ng/mL (Perkin Elmer, Walluf, Germany). Intra-assay variability (coefficients of variation) of the samples was below 10%.

Clinical study

In vivo patient cohort

One hundred and ten treatment naïve MS patients (76 females, age = 38.4 ± 2.4 years, disease duration = 2.8 ± 4.5 years) were enrolled at the time of diagnosis at the MS Centre of the Verona University Hospital. Patients underwent a CSF withdrawal by lumbar puncture, a neurological evaluation including the measure of the Expanded Disability Status Scale (EDSS)³² (median EDSS = 2, range 0–4), a 3T MRI scan, and a neuropsychological assessment. The study was approved by the Ethics Committee of the University of Verona and informed consent was collected from all participants (MSBioB Biological bank – A.O.U.I, Verona; Protocol number 66418, 25/11/2019).

CSF analysis

CSF levels of PVALB and Nf-L were measured using a Parvalbumin ELISA kit (MBS2022353, MyBioSource) and Human Nf-L ELISA kit (MyBioSource), respectively, as described above. PVALB and Nf-L levels were also evaluated in the CSF of 32 control subjects (Suppl. Materials).

MRI acquisition and analysis

Three tesla MRI was performed at the Radiology unit of the Verona University Hospital (Italy) by using a Philips Achieva 3T MR Scanner. The acquisition protocol consisted of: (1) a 3D T1 weighted Turbo Field Echo (TFE) (Repetition Time (TR) / Echo Time (TE) = 8.4/3.7 msec, voxel size of $1 \times 1 \times 1$ mm), total acquisition time of 5:51 min; (2) a 3D Double Inversion Recovery (DIR) (TR/TE = 5500/292 msec, Inversion Times (TI) TI1/TI2 = 525/2530 msec voxel size of $1 \times 1 \times 1$ mm), Turbo Spin Echo (TSE) readout, number of excitations 3, acquisition time of 10:49 min; (3) a 3D Fluid Attenuated Inversion Recovery (FLAIR) (TR/TE = 8000/292 msec, TI = 2350 msec voxel size of $1 \times 1 \times 1$ mm), same TSE readout as the DIR sequence, number of excitations 1, acquisition time of 4:50 min. The acquired images were analyzed to assess the lesion load both in white and grey matter. WM lesions were identified and segmented on FLAIR images using a semiautomatic lesion segmentation technique included in MIPAV (Medical Image Processing and Visualization; mipav.cit.nih.gov) software. The number of cortical lesions (CLs) was assessed on DIR images following the recent recommendations for cortical lesions scoring in patients with MS.³³ Owing to the suboptimal performance of the image-acquisition sequences on MRI in visualizing subpial lesions, the present analysis has taken into account mainly the intracortical and leukocortical lesions. Global and regional cortical thickness evaluation was performed on the 3D T1w scan by using the Freesurfer image analysis suite, available online (<http://surfer.nmr.mgh.harvard.edu/>), as previously described.³⁴ All images were accurately controlled for errors/artefacts by an experienced neurologist (MC) and defects due to tissue lesions were corrected using a semi-automated procedure involving lesions filling.

Neuropsychological assessment

Neuropsychological assessment was available in a subgroup of 93 out of 110 MS patients (85% of the whole sample). The battery of neuropsychological tests was composed of the Brief Repeatable Battery³⁵ (BRB) and the Stroop Test³⁶ (ST). Scores below the cut-off (5th percentile) of the reference population of each test were classified as failed test. MS patients were classified as being cognitively normal (CN, 0 failed subtest) or as having mild cognitive impairment (mCI, up to two failed subtests) or severe cognitive impairment (sCI, at least three failed subtests) considering their performance on all neuropsychological tests administered (for the same procedure, see Pitteri *et al.*, 2017).³⁷

A

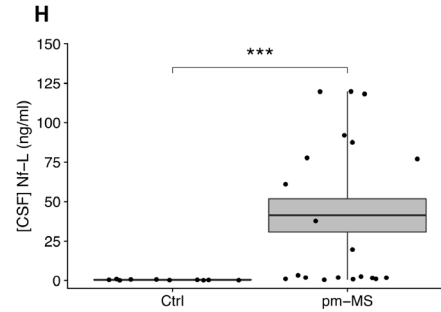
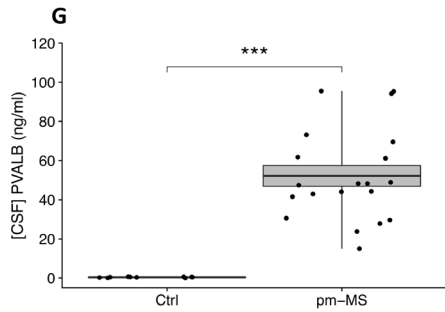
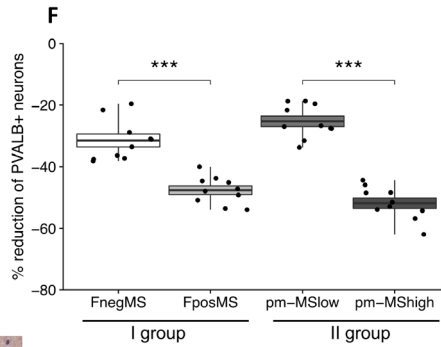
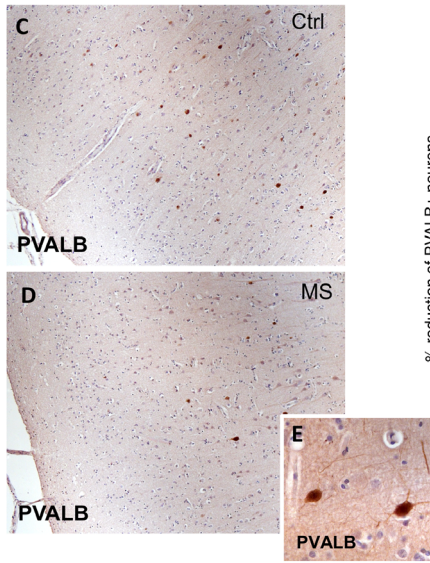
Top 5 Biological processes

#term ID	term description	FDR
GO:0051049	regulation of transport	0.0018
GO:0007422	peripheral nervous system development	0.002
GO:0022008	neurogenesis	0.002
GO:0030182	neuron differentiation	0.002
GO:0007399	nervous system development	0.0026

B

Top 5 Molecular functions

#term ID	term description	FDR
GO:0005251	delayed rectifier potassium channel activity	0.0111
GO:0005244	voltage-gated ion channel activity	0.0157
GO:0005249	voltage-gated potassium channel activity	0.0157
GO:0015077	monovalent inorganic cation transmembrane transporter activity	0.0157
GO:0030550	acetylcholine receptor inhibitor activity	0.0157



I

	CSF PVALB (ng/ml)	CSF Nf-L (ng/ml)
CSF PVALB (ng/ml)		0.38
CSF Nf-L (ng/ml)	0.38	
PVALB+ cell counts	-0.64**	-0.37
% GM demyelination	0.66**	0.21
MHC-II+ cell counts	0.74***	0.09
Age of onset	-0.49*	-0.45*
Age at wheelchair	-0.49*	-0.09
Disease duration	0.18	0.17
Age of death	-0.65**	-0.26

Statistical analysis

Statistical analyses were performed using GraphPad Prism 5 software (GraphPad, La Jolla, CA, USA), R (<https://www.r-project.org/>, version 3.3), and SPSS statistic (SPSS Inc, Chicago, Illinois, USA, version 24) programs. R, Cytoscape (version 3.7.1) and Inkscape (version 0.92.4) were used to draw graphs. For bioinformatic analyses, modified Fisher's exact P value (EASE) was used to determine the gene-enrichment analysis and Benjamini-Hochberg multiple test correction to calculate the false discovery rate (FDR). Shapiro-Wilk test was used to assess the data distribution. Difference between groups were evaluated performing Mann-Whitney test and one-way analysis of variance (one-way ANOVA) followed by post-hoc Tukey test.

Pairwise univariate Spearman rank index was used to evaluating the association between demographical, clinical, neuroradiological, neuropsychological parameters and the CSF PVALB/Nf-L. We tested multiple regression analyses to find which CSF-biomarkers among PVALB and Nf-L better explained each neuroimaging feature. Collinearity was checked by Variance Inflation Factors. Regression diagnostic was used in order to explore the model's statistical assumptions: homoscedasticity and normality of residuals visual inspections did not show important deviations. CSF levels were log transformed to approximate a normal distribution as well as to obtain reliable Beta estimates.

A hierarchical regression model was performed to better explain the amount variance of mean global CTh combining CSF PVALB and CSF Nf-L.

Correlations between CSF PVALB/Nf-L levels and PVALB+ cell counts, % GM demyelination, MHC-II+ cell counts were evaluated using pairwise univariate Pearson coefficient. A false discovery rate (FDR) correction was applied. Unless otherwise indicated, mean \pm SEM was provided for post-mortem data considering the smaller sample, while mean \pm SD was provided for in-vivo data. A *P*-value less than 0.05 was considered significant.

Results

Post-mortem tissue study

Downregulation of PVALB gene in MS reflects reduction of PVALB+ cells in post-mortem tissue of MS brains

We selected the most de-regulated genes expressed in GM lesions of the motor cortex derived from Fpos SPMS (GML_Fpos) cases respect to controls (Fold Change > 2, $P < 0.01$; Fig. S1A and B) from our previously reported gene expression dataset²⁵ and performed gene ontology enrichment analyses. Most of the selected genes are localized in neurons and involved in neuron-associated biological processes (Fig. 1A) and molecular functions (Fig. 1B), such as neuron differentiation and voltage-gated ion channel activity. Accordingly, the most enriched cellular component clusters were related to neuronal processes such as axons and neuron projections (Fig. S1A). Protein-protein interaction analysis revealed a core network particularly enriched in "neuron part" cluster (Fig. S1E). The expression of these neuronal genes was investigated in our three other datasets (NAGM_FPOS: normal appearing GM in follicle-positive SPMS cases; GML_Fneg: GM lesions in follicle-negative SPMS cases; NAGM_Fneg: normal appearing GM in follicle-negative SPMS cases).²⁵ PVALB was the most downregulated gene (fold change = 3.7 ± 1.2 , $P < 0.00$) in both GML and NAGM of Fpos cases, whereas Fneg cases showed a very different overall expression pattern for the genes of interest (Fig. S1B).

PVALB expressing interneuron numbers are substantially reduced in MS cortex

Quantitative analysis of the density of PVALB+ cells (Fig. 1E) in the motor cortex of the control (Fig. 1C) and MS (Fig. 1D) cases, revealed a significant ($P < 0.0001$)

Figure 1. Molecular and neuropathology analysis of PVALB expression in post-mortem progressive MS. Gene ontology enrichment analysis for the top five biological process (A) and molecular function (B) clusters of differentially expressed genes in post-mortem precentral gyrus with grey matter (GM) lesions derived from SPMS cases characterized by the presence follicle-like structures (Fpos). A modified Fisher's exact *P*-value (EASE) was used to determine the gene-enrichment analysis and Benjamini-Hochberg multiple test correction was applied to calculate the False Discovery Rate (FDR). Immunohistochemical assessment of PVALB+ cells in the precentral gyrus (motor cortex) of one post-mortem control (C) and one MS case (D). PVALB immunostaining detected a subpopulation of cortical neurons (E). (F) Boxplot reporting the percentage reduction of PVALB+ cells with respect to control in post-mortem precentral gyrus of the two independent MS cohorts (group I and II). (G) PVALB protein levels in available paired CSF post-mortem samples ($n = 20$) and age-matched healthy controls ($n = 10$). (H) Nf-L protein levels in available paired CSF post-mortem samples ($n = 20$) and age-matched healthy controls ($n = 10$). (I) Summary table of the correlation analyses between PVALB/Nf-L CSF levels and PVALB+ cell counts, % GM demyelination, MHC-II+ cell counts, age of disease onset (years), age at wheelchair (years; EDSS = 7), disease duration (years), and age at death (years). Means and SEM were used to represent the data. Dots represent the samples analyzed. * $P < 0.05$; ** $P < 0.01$; *** $P < 0.001$. pm-MS: post-mortem Multiple Sclerosis cases; Ctrl: controls; *R*: correlation coefficient; *P*: *P*-value; GM: grey matter; MHC-II: major histocompatibility complex-II. Original magnifications: A, B 100 \times ; B, D 400 \times .

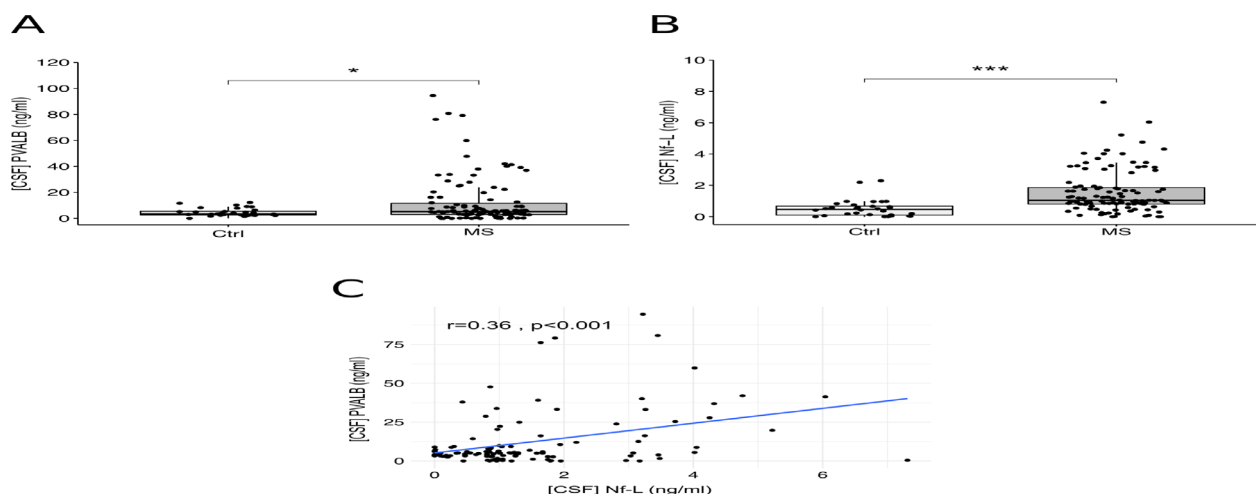


Figure 2. Increased CSF PVALB and Nf-L levels in MS patients. (A) PVALB protein concentration in CSF from controls ($n = 32$) and MS patients ($n = 110$). (B) Nf-L protein concentration in CSF from controls ($n = 32$) and MS patients ($n = 110$). (C) Correlation between CSF PVALB and Nf-L levels in MS patients ($r = 0.036$, $P < 0.001$, $n = 110$). Boxplots show the medians and the two hinges. Dots represent the samples analyzed. * $P < 0.05$, *** $P < 0.001$. MS: Multiple Sclerosis; Ctrl: controls; r : Pearson correlation coefficient; P : P -value.

reduction of PVALB⁺ cell density in follicle-positive (Fpos) MS cases (51.6%) and follicle-negative (Fneg) MS cases (25.3%) with respect to controls (Fig. 1F). In addition, PVALB⁺ cell density reduction was significantly higher in Fpos respect to Fneg cases (Fig. 1F). Similarly, a significant ($P < 0.0001$) reduction of PVALB⁺ cell density was measured in the motor cortex of the second, independent, post-mortem MS group, in both *MShigh* cases (47.6%; $P < 0.0001$) and *MSlow* cases (31.5%; $P < 0.0001$) with respect to controls (Fig. 1F). In addition, PVALB⁺ cell density reduction was significantly higher in *MShigh* respect to *MSlow* cases (Fig. 1F).

PVALB protein levels are significantly elevated in post-mortem CSF

Analysis of PVALB protein levels in the available paired CSF samples of the post-mortem MS and control cases demonstrated significantly higher levels in MS (mean \pm SEM = 64.3 ± 8.2 ; $P < 0.0001$) compared to controls (mean \pm SEM = 0.32 ± 0.06) (Fig. 1G). Similarly, significantly increased CSF Nf-L levels were found in MS (mean \pm SEM = 81.01 ± 10.8 ; $P < 0.0001$) compared to controls (mean \pm SEM = 0.34 ± 0.07) (Fig. 1H). There was a modest correlation between CSF levels of PVALB and Nf-L ($r = 0.38$; $P = 0.09$).

When CSF PVALB and Nf-L levels were compared with cell counts performed in the same MS cases, PVALB levels correlated negatively with PVALB cell counts ($r = -0.64$; $P < 0.01$) and positively with % of GM demyelination ($r = 0.66$; $P < 0.01$) and numbers of activated microglia/macrophages ($r = 0.74$; $P < 0.01$)

examined in the same areas (Fig. 1I). There was also a significant negative correlation between CSF PVALB levels and age of onset ($r = -0.46$; $P < 0.05$), age at wheelchair use ($r = -0.50$; $P < 0.05$) and age at death ($r = -0.65$; $P < 0.01$), but not with disease duration (Fig. 1I). In contrast, a significant negative correlation was only found between Nf-L CSF levels and age of onset ($r = -0.46$; $P < 0.05$) (Fig. 1I).

Patient cohort study

CSF PVALB is increased in MS at the time of diagnosis

Significantly increased PVALB levels were present in the CSF of MS patients (fold change = 3.0 ± 2.1 , $P = 0.002$) when compared to the control cohort (Fig. 2A). Likewise, a significant increase of Nf-L levels was found in the CSF of MS patients (fold change = 3.5 ± 1.3 , $P < 0.001$) compared to controls (Fig. 2B). The levels of PVALB and Nf-L in post-mortem CSF samples (PVALB mean \pm SEM = 42.4 ± 5.2 ; Nf-L mean \pm SEM = 81.0 ± 6.4 ng/mL) were substantially higher compared to those in naïve MS patients at diagnosis, as expected (PVALB mean \pm SD = 5.2 ± 8.3 ng/mL; Nf-L median \pm SD = 1.0 ± 1.3 ng/mL). There was a significant positive correlation between CSF levels of PVALB and Nf-L ($r = 0.36$, $P < 0.001$) (Fig. 2C). On the contrary, no significant correlation was found between PVALB (and Nf-L) levels and age, disease duration, gender, and EDSS. Moreover, no significant correlation was found between EDSS and WM lesion number.

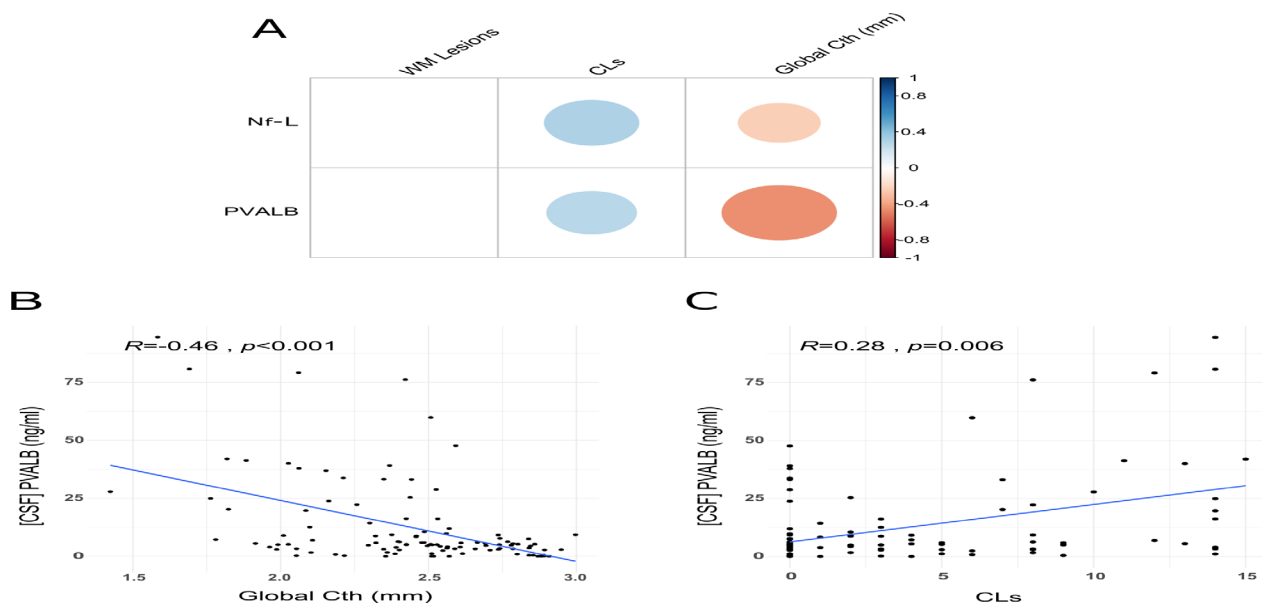


Figure 3. 3T MRI global outcomes correlations with CSF PVALB and Nf-L levels in MS patients. (A) Correlation plot showing different strength of correlation between CSF PVALB and Nf-L levels with MRI parameters. A false discovery rate (FDR) correction was applied. The Spearman rank index is proportional to the dimension/intensity of the bubbles. A color scale was used to determine the slope of the correlation. Blank squares indicate no significant correlation. (B) Scatter plot of relationship between CSF PVALB levels and global cortical thickness (CTH) in MS patients. (C) Scatter plot of relationship between CSF PVALB levels and number of cortical lesions (CLs) in MS patients. Dots represent the samples analyzed. CLs: cortical lesions; CTh: cortical thickness; R : Spearman correlation coefficient; P : P -value.

Increased PVALB levels are associated with cortical damage

The global CTh (mean \pm SD = 2.44 ± 0.34 mm, range 1.42–3.00 mm) correlated moderately with CSF PVALB levels ($R = -0.46, P < 0.001$) and only slightly with Nf-L levels ($R = -0.23, P = 0.024$) (Fig. 3A, C and D and Table S2). The global CTh was found to be associated with CSF PVALB levels in a partial correlation controlling for the number of CLs ($r = -0.32, P = 0.001$).

Furthermore, two nested regression models were assessed using global CTh as dependent variable: the first model (model-1) included only the CSF Nf-L variable and in the next step (model-2) CSF PVALB was added. Then, ANOVA analysis was applied to compare the two models by Sum of Square (SS) and R^2 . Model-1 revealed that CSF Nf-L was associated with the Global CTh ($\beta = -0.12, P = 0.005, R^2 = 0.07$) but by adding the CSF PVALB the variance of Global CTh was explained only by CSF PVALB (CSF PVALB $\beta = -0.09, P < 0.001$, CSF Nf-L, $P = 0.09$ and $R^2 = 0.26$). Model-2 accounts for additional SS = 2.3 and the R^2 increased by 0.19 ($P < 0.001$).

Moreover, the number of CLs (mean \pm SD = 3.88 ± 5.00 , range 0–23) was slightly correlated with CSF PVALB levels ($R = 0.28, P = 0.006$) and with Nf-L levels ($R = 0.31, P = 0.003$), whereas WM lesion number (mean \pm SD = 8.79 ± 3.99 , range 0–19) did not

correlate with CSF levels of PVALB (Fig. 3B) or Nf-L. Regression models confirmed these results. In fact, the analysis revealed that unlike Nf-L levels, CSF PVALB levels were associated with global CTh ($\beta = -0.09, P < 0.001$). Also, both CSF PVALB and Nf-L levels were related to the CL load (PVALB: $\beta = 0.89, P = 0.001$; Nf-L: $\beta = 2.26, P < 0.001$). Finally, like univariate correlation analysis, multivariate regression showed that neither CSF PVALB nor Nf-L levels were linked to WM lesion number.

Increased PVALB levels are associated with fronto-temporal thinning

The regional analysis revealed that PVALB was significantly associated with CTh of several brain regions (Fig. 4A and Table 2); in particular, using both correlation analysis and regression models, PVALB strongly correlated with the CTh of insula (correlation: $R = -0.55, P < 0.001$; regression: $\beta = -0.62, P < 0.001$), cingulate gyrus ($R = -0.47, P < 0.001, \beta = -0.36, P < 0.05$), hippocampus ($R = -0.46, P < 0.001, \beta = -0.31, P < 0.001$), post-central gyrus ($R = -0.46, P < 0.001, \beta = -0.22, P < 0.001$), parahippocampal gyrus ($R = -0.43, P < 0.001, \beta = -0.30, P < 0.01$), middle temporal gyrus ($R = -0.42, P < 0.001, \beta = -0.36, P < 0.01$), and superior frontal gyrus ($R = -0.42, P < 0.001, \beta = -0.22,$

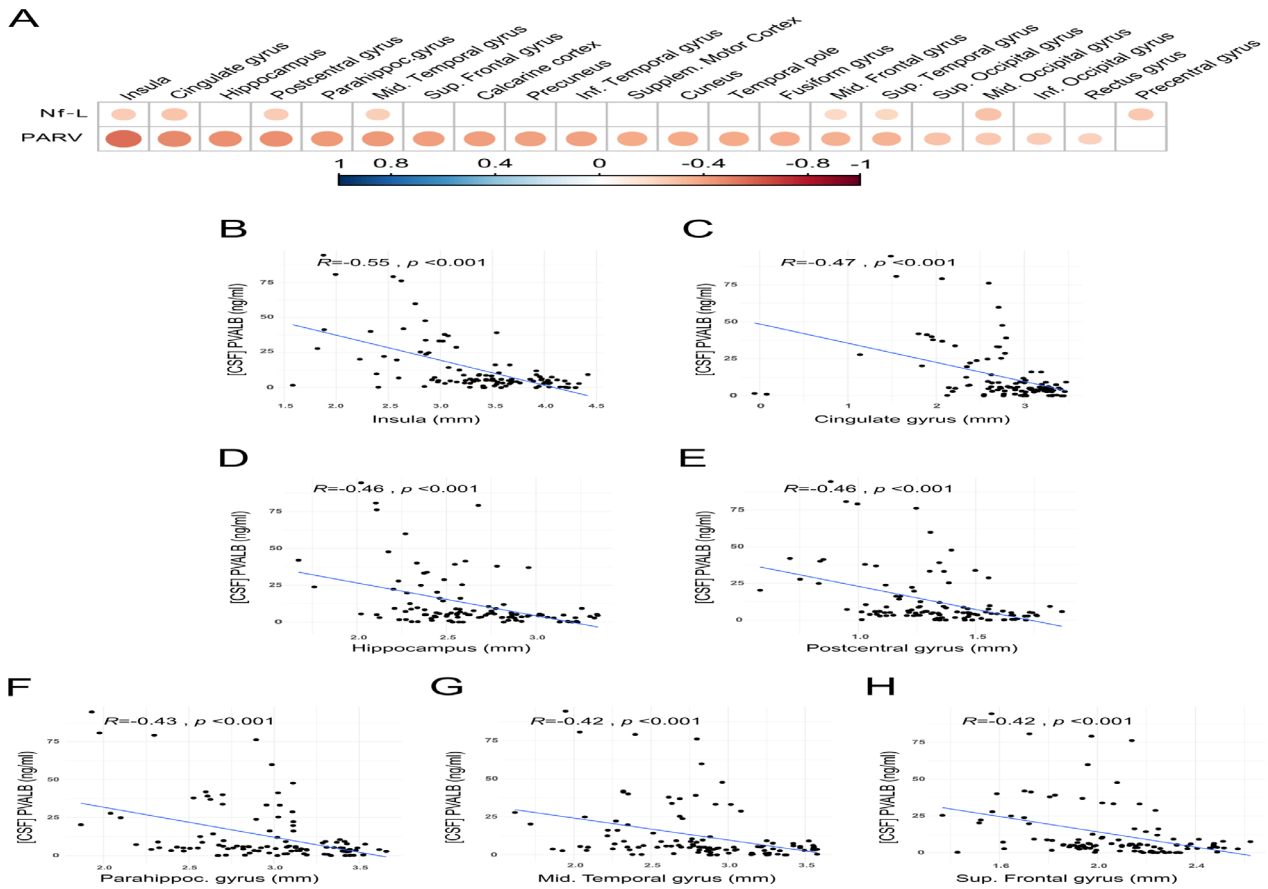


Figure 4. CSF PVALB levels correlations with 3T-MRI regional CTh in MS patients. (A) Correlation plot chart showing the correlation between PVALB levels and Nf-L with regional cortical thicknesses. A false discovery rate (FDR) correction was applied. The Spearman rank index is proportional to the dimension/intensity of the bubbles. A color scale was used to determine the slope of the correlation. Blank squares indicate no significant correlation. (B–H) Scatter plot of relationship between CSF PVALB levels and CTh of the most associated brain regions: (B) insula, (C) cingulate gyrus, (D) hippocampus, (E) postcentral gyrus, (F) parahippocampal gyrus, (G) middle temporal gyrus, (H) superior frontal gyrus. Dots represent the samples analyzed. *R*: Spearman correlation coefficient; *P*: *P*-value.

$P < 0.001$) (Fig. 4B–H). See Table 3 for multiple regression analysis. In contrast, only few significant correlations were found between Nf-L levels and regional CTh levels (Fig. 4A; Fig. S3).

CSF PVALB is increased in patients with severe global cognitive impairment

Thirty-nine (42%) of the 93 MS patients who underwent the neuropsychological assessment were classified as being cognitively normal (CN), 39 (42%) as having mild cognitive impairment (mCI), and 15 (16%) as having severe cognitive impairment (sCI). PVALB levels were significantly different among the three groups ($P = 0.026$): post-hoc analyses showed no significant difference between CN and mCI ($P = 0.508$) groups, while patients with sCI were characterized by a significant increase of PVALB levels (mean \pm SEM = 25.2 \pm 7.5 ng/mL)

compared to both CN (mean \pm SEM = 10.9 \pm 2.4 ng/mL, $P = 0.049$) and mCI (mean \pm SEM = 10.1 \pm 2.9 ng/mL, $P = 0.024$) patients (Fig. 5A). On the contrary, no significant difference was observed for Nf-L levels among the three subgroups ($P = 0.220$) (Fig. 5B).

Discussion

In the present study, we investigated the extent of the loss of PVALB+ GABAergic interneurons in the motor cortex of post-mortem MS cases compared to controls and provided a possible link with increased PVALB levels in the CSF from the same cases. Our data strongly suggest that CSF protein levels of PVALB reflect loss of GABAergic interneurons in MS cortex in progressive MS at the time of death. By combining CSF and 3T-MRI analyses in a cohort of MS patients at the time of diagnosis, together

Table 2. Correlations between global and regional CTh with both CSF PVALB and Nf-L levels in MS patients.

CTh	PVALB	Nf-L
Global CTh	-0.46 ($P < 0.001$)	-0.23 ($P = 0.024$)
Insula	-0.55 ($P < 0.001$)	-0.24 ($P = 0.012$)
Cingulate gyrus	-0.47 ($P < 0.001$)	-0.27 ($P = 0.005$)
Hippocampus	-0.46 ($P < 0.001$)	n.s.
Postcentral gyrus	-0.46 ($P < 0.001$)	-0.24 ($P = 0.010$)
Parahippocampal gyrus	-0.43 ($P < 0.001$)	n.s.
Middle temporal gyrus	-0.42 ($P < 0.001$)	-0.24 ($P = 0.014$)
Superior frontal gyrus	-0.42 ($P < 0.001$)	n.s.
Calcarine cortex	-0.42 ($P < 0.001$)	n.s.
Precuneus	-0.40 ($P < 0.001$)	n.s.
Inferior temporal gyrus	-0.40 ($P < 0.001$)	n.s.
Supplementary motor cortex	-0.39 ($P < 0.001$)	n.s.
Cuneus	-0.38 ($P < 0.001$)	n.s.
Temporal pole	-0.37 ($P < 0.001$)	n.s.
Fusiform gyrus	-0.37 ($P < 0.001$)	n.s.
Middle frontal gyrus	-0.35 ($P < 0.001$)	-0.20 ($P = 0.044$)
Superior temporal gyrus	-0.34 ($P < 0.001$)	-0.20 ($P = 0.032$)
Superior occipital gyrus	-0.29 ($P = 0.002$)	n.s.
Middle occipital gyrus	-0.27 ($P = 0.006$)	-0.28 ($P = 0.003$)
Inferior occipital gyrus	-0.25 ($P = 0.009$)	n.s.
Rectus gyrus	-0.22 ($P = 0.021$)	n.s.
Precentral gyrus	n.s.	-0.26 ($P = 0.007$)

Spearman correlation coefficients and P -values (in brackets) are listed in a decrescent order of association with PVALB.

with clinical and neuropsychological data, we found that the CSF protein level of PVALB could represent a new biomarker of GM damage, in particular of GM atrophy and associated cognitive decline.

PVALB as a new biomarker of interneuronal loss at early disease stage

Similar to other CSF biomarkers thought to reflect activity or damage associated with MS pathology and released into the CSF,³⁸ PVALB is most likely released into the CSF as a consequence of interneuronal loss. Compared to Nf-L, our results show that CSF PVALB levels correlate better with cortical thinning and cognitive impairment than Nf-L and also earlier, at the time of diagnosis. In particular, CSF Nf-L levels were found to have a stronger association with cortical lesion number at baseline compared to the other examined MRI and clinical parameters. On the contrary, PVALB CSF levels correlated, not only with cortical lesion number but also with global and regional cortical thinning, suggesting that it could represent a more specific marker of cortical neurodegeneration-related atrophy.

These findings suggest that PVALB, by reflecting the interneuron loss in the cortex, may represent primarily a

Table 3. Results from the several regression models. For each regression analysis, β coefficient and P -value of CSF PVALB and Nf-L were reported.

CTh regional	PVALB		Nf-L	
	β coefficient	P -value	β coefficient	P -value
Insula	-0.63	***	-0.38	*
Cingulate gyrus	-0.36	*	-0.41	*
Hippocampus	-0.31	***	/	n.s.
Postcentral gyrus	-0.22	***	/	n.s.
Parahippoc. gyrus	-0.30	**	/	n.s.
Mid. Temporal gyrus	-0.36	**	/	n.s.
Sup. Frontal gyrus	-0.22	***	/	n.s.
Calcarine coretex	-0.46	***	/	n.s.
Precuneus	-0.32	**	/	n.s.
Inf. Temporal gyrus	-0.20	0.07.	/	n.s.
Supplem. Motor Cortex	-0.30	***	/	n.s.
Cuneus	-0.23	*	/	n.s.
Temporal	-0.33	***	/	n.s.
Fusifrom gyrus	-0.28	*	/	n.s.
Mid. Frontal gyrus	-0.25	**	/	n.s.
Sup. Temporal pole	-0.21	***	/	n.s.
Sup. Occipital gyrus	-0.16	0.06	/	n.s.
Mid. Occipital gyrus	/	n.s.	-0.26	*
Inf. Occipital gyrus	-0.19	0.07.	/	n.s.
Rectus gyrus	-0.49	***	/	n.s.
Precentral gyrus	/	n.s.	-0.19	0.05

n.s. = not significant.

* $P < 0.05$.

** $P < 0.01$.

*** $P < 0.001$.

biomarker of specific cortical neurodegeneration that is independent from cortical demyelination. Our results are consistent with other studies suggesting that cortical thinning is independent of demyelination (29; Wegner et al., 2006; 14; 17). In particular, in line with previous data,²⁹ we measured a similar reduction of PVALB gene expression and PVALB-positive neuronal loss both in GM lesions and normal appearing GM of post-mortem MS cases compared to controls. It has been suggested that in chronic demyelination in the MS cortex, microglia may be intimately associated with neuronal perikarya and proximal dendrites and may mediate axonal degeneration even in normal-appearing GM.¹⁶ The finding that high levels of PVALB may be detected in MS patients at the time of diagnosis and correlate with cortical thinning more than cortical lesion load highly supports the hypothesis that neurodegeneration might be independent of cortical demyelination and can be estimated by MRI analysis of cortical thickness changes in combination with CSF assessment of PVALB levels. The fact that PVALB

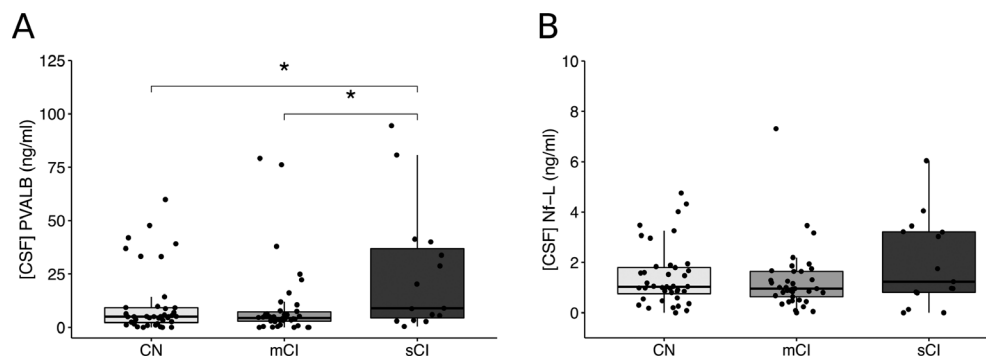


Figure 5. Correlations between cognitive impairment and global cortical thickness and with CSF PVALB and NF-L levels in MS patients. (A) Boxplot representing the comparison of PVALB levels among the MS groups characterized by different levels of cognitive impairment. (B) Boxplot representing the comparison of NF-L level among the MS groups characterized by different levels of cognitive impairment. Boxplots show the medians and the two hinges. Dots represent the individual samples analyzed. * $P < 0.05$. CTh: cortical thickness; CN: cognitively normal MS patients; mCI: MS patients with mild cognitive impairment; sCI: MS patients with severe cognitive impairment.

and Nf-L levels in post-mortem CSF samples were substantially higher than in drug-naïve MS patients, may imply that the level of interneuronal damage may be low in early disease stages and may then slowly increase as MS progresses. Assessment of PVALB CSF levels in follow-up studies would possibly clarify whether this biomarker reflects the increase of neurodegeneration over time.

Loss of PVALB-positive interneurons is associated with intrathecal inflammation

We found that the reduction of PVALB-positive neurons is strictly associated with the density of activated microglia in the same area and this is particularly elevated in MS patients with meningeal lymphoid-like structures. In some of these patients, we previously identified a “surface-in” gradient of microglial activation, higher in the most external cortical layers close to the pial surface and reduced close to the WM. The results of the present study support the hypothesis that meningeal inflammation may mediate and/or enhance cortical neurodegeneration possibly by regulating/inducing subpial microglia activation.⁷ The fact that we found in-vivo CSF PVALB levels early in the disease course, suggests that PVALB can be considered as a biomarker of active cortical pathology, both in GM lesions and in normal appearing GM.

The results from both post-mortem tissue and patient studies confirm a key role for meningeal inflammation in cortical damage and neurodegeneration. The finding of higher loss of PVALB-positive neurons and the corresponding increase in CSF levels in post-mortem MS cases with meningeal lymphoid-like immune cell infiltrates, as well as in the second independent *MShigh* population with increased level of diffuse meningeal inflammation,

supports the hypothesis that inflammation, compartmentalized in the meninges, may contribute not only to GM demyelination but also to neurodegeneration. These data are strongly supported by the recent single-nucleus RNA sequencing study in multiple cell lineages in MS lesions, showing high vulnerability of upper-cortical-layer neurons and reactive glia at the borders of subcortical MS lesions associated with progression in MS.¹⁸

PVALB represents a biomarker of cortical damage in early MS

In our study, we found a moderate significant correlation between PVALB concentration in the CSF and the reduction of cortical thickness, but not with WM demyelination. Our analyses demonstrated that CSF-PVALB variable may play a key role in explaining the variance of Global CTh. This finding was particularly evident in certain cortical regions, such as insula, cingulate gyrus, hippocampus, postcentral gyrus, parahippocampal gyrus, middle temporal gyrus, and superior frontal gyrus, which were all previously identified by both neuropathological and MRI studies.^{7,31,39–41} as severely affected by cortical pathology. These cortical regions, similar to the motor cortex, in which a reduction of PVALB gene expression and GABA-ergic interneurons have been observed, seem to be the most susceptible to neurodegeneration at least in the early stage of the disease. Previous studies hypothesized that the effect of meningeal inflammation was stronger in those regions of the cortex with deep invaginations and low CSF flow, such as insula and cingulate gyrus.^{41,42} In our study, these regions seemed to be highly correlated with the CSF PVALB values supporting, from an MRI point of view, the association between meningeal inflammation and neurodegeneration.

PVALB as potential prognostic biomarker of more severe disease outcome in progressive MS

The post-mortem MS cases with an increased degree of meningeal inflammation and cortical pathology were characterized by a more severe and rapid disease progression¹⁵ and by the most extensive interneuronal loss together with high CSF levels of PVALB. The negative correlations identified between CSF PVALB levels and both age of onset and age of death of these post-mortem cases suggest an inflammation-driven neurodegeneration mechanism that possibly is linked to early and more severe disease (early age of death). In the early relapsing remitting phase of the naïve MS patients, we did not find significant correlations between PVALB CSF levels and clinical parameters, such as EDSS. This is possibly due to either to the cortical plasticity, that allows good compensatory mechanisms and that accumulation of neurodegeneration plays a role mainly in the progressive disease phase,⁴³ or to the prevalent involvement of white matter lesions in the initial disease outcome.

PVALB, a biomarker associated with cognitive dysfunction

The high PVALB CSF level observed in patients with severe CI suggests that PVALB could be a valuable biomarker of cognitive dysfunction related to cortical pathology since the early phase of the disease. This is in line with previous studies showing a relationship between CI and GM damage rather than with WM damage.⁴⁴ We also observed that PVALB is more correlated with CTh respect to CLs, thus suggesting that CI is more associated with diffuse GM neuronal and interneuronal loss than focal cortical GM damage, which seems to be mainly captured by the Nf-L CSF level. Although CSF Nf-L might reflect CI in MS patients even in the earliest phases of the disease,^{45–47} it should not be considered as a biomarker specific for CI, since its levels in the CSF increase as an expression of axonal damage, which in turn may be the basis of the involvement of functional systems other than the cognitive one.⁴³ This observation can also contribute to explain why PVALB is more associated with cognitive rather than physical (measured by EDSS) disability. The present results may suggest that PVALB might be more sensitive than Nf-L in detecting CI since the earliest phase of the disease because its association with both neuronal and interneuronal loss in the GM. Extending this study to a larger and independent MS population, and integrating a long follow-up period of combined clinical, radiological, and neuropsychological analysis, could reveal the role of PVALB as a potential better predictive biomarker, with

respect to Nf-L, either of cognitive decline or of worst brain atrophy in the long-term disease course.

Conclusions

By combining a molecular neuropathology, MRI, clinical, and neuropsychological approach, we have shown that CSF PVALB levels represent a new potential biomarker of interneuron loss in the cortex of MS patients, both at time of diagnosis and, increasing with progression, at time of death. In particular, this biomarker is able to reflect early alterations in cortical thickness and cognitive impairment, not revealed from assessment of CSF Nf-L levels and may, therefore, be useful to more efficiently recognize MS patients that present with early signs of neurodegeneration and related cognitive decline enabling treatment with specific combinations of neuroprotective and immunomodulatory treatments.

Acknowledgments

Magliozzi and Tamanti were supported by Italian MS Foundation grant (FISM 16/17/F14). Calabrese and Rossi were supported by the GR-2013-02-355322 grant from Italian Ministry of Health. Reynolds and Nicholas were supported by the MS Society of Great Britain and Northern Ireland (grant 910/09), the National Institute for Health Research Biomedical Research Centre at Imperial College and the EU 6th Framework Network of Excellence BrainNetEurope II.

Conflict of Interest

The authors declare that there is no conflict of interest.

Author Contributions

RM, MP, RR, and MC contributed to the conception and design of the study; RM, MP, SZ, DM, LM, SR, MG, CD, AIP, RN, RR, and MC contributed to the acquisition and analysis of data; RM, MP, RN, RR, and MC contributed to data interpretation and discussion; RM, MP, SZ, DM, LM, SR, VM, GMS, AIP, RN, RR, and MC contributed to write and revise the manuscript.

Study Approval

Biological material and associated data were obtained from MSBioB Biological bank - A.O.U.I, Verona (Protocol number 66418, 25/11/2019). Biological material was obtained from voluntary donors in compliance with the Legislative Decree 196/2003 “Personal Data Protection Code”.

All post-mortem tissues were obtained from the UK MS Society Tissue Bank at Imperial College and were obtained at autopsy with fully informed consent under ethical approval by the National Research Ethics Committee (08/MRE09/31).

References

- Reynolds R, Roncaroli F, Nicholas R, et al. The neuropathological basis of clinical progression in multiple sclerosis. *Acta Neuropathol* 2011;122:155–170.
- Kutzelnigg A, Lassmann H. Pathology of multiple sclerosis and related inflammatory demyelinating diseases. *Handb Clin Neurol* 2014;122:15–58.
- Noseworthy JH, Lucchinetti C, Rodriguez M, Weinshenker BG. Multiple sclerosis. *N Engl J Med* 2000;343:938–952.
- Calabrese M, Magliozzi R, Ciccarelli O, et al. Exploring the origins of grey matter damage in multiple sclerosis. *Nat Rev Neurosci* 2015;16:147–158.
- Lucchinetti CF, Popescu BF, Bunyan RF, et al. Inflammatory cortical demyelination in early multiple sclerosis. *N Engl J Med* 2011;365:2188–2197.
- Bevan RJ, Rhian E, Griffiths L, et al. Meningeal inflammation and cortical demyelination in acute multiple sclerosis. *Ann Neurol* 2018;84:829–842.
- Calabrese M, Reynolds R, Magliozzi R, et al. Regional distribution and evolution of gray matter damage in different populations of multiple sclerosis patients. *PLoS One* 2015;10:e0135428.
- Rojas JJ, Patrucco L, Miguez J, Cristiano E. Brain atrophy in multiple sclerosis: therapeutic, cognitive and clinical impact. *Arq Neuropsiquiatr* 2016;74:235–243.
- Calabrese M, Poretto V, Favaretto A, et al. Cortical lesion load associates with progression of disability in multiple sclerosis. *Brain* 2012;135:2952–2961.
- Geurts JJ, Calabrese M, Fisher E, Rudick RA. Measurement and clinical effect of grey matter pathology in multiple sclerosis. *Lancet Neurol* 2012;11:1082–1092.
- Chiaravalloti ND, De Luca J. Cognitive impairment in multiple sclerosis. *Lancet Neurol* 2008;7:1139–1151.
- Amato MP, Morra VB, Falautano M, et al. Cognitive assessment in multiple sclerosis—an Italian consensus. *Neurol Sci* 2018;39:1317–1324.
- Charil A, Dagher A, Lerch JP, et al. Focal cortical atrophy in multiple sclerosis: relation to lesion load and disability. *NeuroImage* 2007;34:509–517.
- Magliozzi R, Howell OW, Reeves C, et al. A gradient of neuronal loss and meningeal inflammation in multiple sclerosis. *Ann Neurol* 2010;68:477–493.
- Howell OW, Reeves CA, Nicholas R, et al. Meningeal inflammation is widespread and linked to cortical pathology in multiple sclerosis. *Brain* 2011;134:2755–2771.
- Peterson JW, Bö L, Mörk S, et al. Transected neurites, apoptotic neurons, and reduced inflammation in cortical multiple sclerosis lesions. *Ann Neurol* 2001;50:389–400.
- Klaver R, Popescu V, Voorn P, et al. Neuronal and axonal loss in normal-appearing gray matter and subpial lesions in multiple sclerosis. *J Neuropathol Exp Neurol* 2015;74:453–458.
- Schirmer L, Velmshch D, Holmqvist S, et al. Neuronal vulnerability and multilineage diversity in multiple sclerosis. *Nature* 2019;573:75–82.
- Farina G, Magliozzi R, Pitteri M, et al. Increased cortical lesion load and intrathecal inflammation is associated with oligoclonal bands in multiple sclerosis patients: a combined CSF and MRI study. *J Neuroinflammation* 2017;14:40.
- Magliozzi R, Howell OW, Nicholas R, et al. Inflammatory intrathecal profiles and cortical damage in multiple sclerosis. *Ann Neurol* 2018;83:739–755.
- Salzer J, Svenningsson A, Sundström P. Neurofilament light as a prognostic marker in multiple sclerosis. *Mult Scler* 2010;16:287–292.
- Tiedt S, Duering M, Barro C, et al. Serum neurofilament light: a biomarker of neuroaxonal injury after ischemic stroke. *Neurology* 2018;91:e1338–e1347.
- Feneberg E, Oeckl P, Steinacker P, et al. Multicenter evaluation of neurofilaments in early symptom onset amyotrophic lateral sclerosis. *Neurology* 2018;90:e22–e30.
- Meeter LH, Dopfer EG, Jiskoot LC, et al. Neurofilament light chain: a biomarker for genetic frontotemporal dementia. *Ann Clin Transl Neurol* 2016;3:623–636.
- Magliozzi R, Howell OW, Durrenberger P, et al. Meningeal inflammation changes the balance of TNF signalling in cortical grey matter in multiple sclerosis. *J Neuroinflammation* 2019;16:1–6.
- Hu H, Gan J, Jonas P. Fast-spiking, parvalbumin+ GABAergic interneurons: from cellular design to microcircuit function. *Science* 2014;345:1255–1263.
- Beers DR, Ho BK, Siklós L, et al. Parvalbumin overexpression alters immune-mediated increases in intracellular calcium, and delays disease onset in a transgenic model of familial amyotrophic lateral sclerosis. *J Neurochem* 2001;79:499–509.
- Dekkers J, Bayley P, Dick JR, et al. Over-expression of parvalbumin in transgenic mice rescues motoneurons from injury-induced cell death. *Neuroscience* 2004;123:459–466.
- Dutta R, McDonough J, Yin X, et al. Mitochondrial dysfunction as a cause of axonal degeneration in multiple sclerosis patients. *Ann Neurol* 2006;59:478–489.
- Clements RJ, McDonough J, Freeman EJ. Distribution of parvalbumin and calretinin immunoreactive interneurons in motor cortex from multiple sclerosis post-mortem tissue. *Exp Brain Res* 2008;187:459–465.

31. Magliozzi R, Howell O, Vora A, et al. Meningeal B-cell follicles in secondary progressive multiple sclerosis associate with early onset of disease and severe cortical pathology. *Brain* 2007;130:1089–1104.
32. Kurtzke JF. Rating neurologic impairment in multiple sclerosis: an expanded disability status scale (EDSS). *Neurology* 1983;33:1444–1469.
33. Geurts JJ, Roensdaal SD, Calabrese M, et al. Consensus recommendations for MS cortical lesion scoring using double inversion recovery MRI. *Neurology* 2011;76:418–424.
34. Fischl B, Dale AM. Measuring the thickness of the human cerebral cortex from magnetic resonance images. *Proc Natl Acad Sci USA* 2000;97:11050–11055.
35. Amato MP, Portaccio E, Goretti B, et al. The Rao's Brief Repeatable Battery and Stroop Test: normative values with age, education and gender corrections in an Italian population. *Mult Scler* 2006;12:787–793.
36. Caffarra P, Vezzadini G, Dieci F, et al. Una versione abbreviata del test di Stroop: dati normativi nella popolazione italiana. *Nuova Rivista di Neurologia* 2002;12:111–115.
37. Pitteri M, Romualdi C, Magliozzi R, et al. Cognitive impairment predicts disability progression and cortical thinning in MS: an 8-year study. *Mult Scler* 2017;23:848–854.
38. Magliozzi R, Cross AH. Can CSF biomarkers predict future MS disease activity and severity? *Mult Scler* 2020;6:582–590.
39. Wegner C, Esiri MM, Chance SA, et al. Neocortical neuronal, synaptic, and glial loss in multiple sclerosis. *Neurology* 2006;67:960–967.
40. Kutzelnigg A, Lucchinetti CF, Stadelmann C, et al. Cortical demyelination and diffuse white matter injury in multiple sclerosis. *Brain* 2005;128:2705–2712.
41. Frischer JM, Bramow S, Dal-Bianco A, et al. The relation between inflammation and neurodegeneration in multiple sclerosis brains. *Brain* 2009;132:1175–1189.
42. Haider L, Zrzavy T, Hametner S, et al. The topography of demyelination and neurodegeneration in the multiple sclerosis brain. *Brain* 2016;139:807–815.
43. Eshaghi A, Prados F, Brownlee WJ, et al. Deep gray matter volume loss drives disability worsening in multiple sclerosis. *Ann Neurol* 2018;83:210–222.
44. Scott TF. Understanding the impact of relapses in the overall course of MS; refinement of the 2 stage natural history model. *J Neuroimmunol* 2017;305:162–166.
45. Rocca MA, Amato MP, De Stefano N, et al. Clinical and imaging assessment of cognitive dysfunction in multiple sclerosis. *Lancet Neurol* 2015;14:302–317.
46. Quintana E, Coll C, Salavedra-Pont J, et al. Cognitive impairment in early stages of multiple sclerosis is associated with high cerebrospinal fluid levels of chitinase 3-like 1 and neurofilament light chain. *Eur J Neurol* 2018;25:1189–1191.
47. Gaetani L, Salvadori N, Lisetti V, et al. Cerebrospinal fluid neurofilament light chain tracks cognitive impairment in multiple sclerosis. *J Neurol* 2019;266:2157–2163.

Supporting Information

Additional supporting information may be found online in the Supporting Information section at the end of the article.

Figure S1. Gene expression analysis in post-mortem tissue of MS patients.

Figure S2. 3T MRI global outcomes correlations with CSF Nf-L levels in MS patients.

Figure S3. CSF Nf-L levels is low associated with 3T MRI CTh of brain regions in MS patients.

Table S1. Expression data of genes belonging to "Neuron part" cluster in GO analysis for Cellular Component (CC) (data obtained from Magliozzi *et al.*).

Table S2. Hierarchical regression model performed to explain the amount variance of mean global CTh combining CSF PVALB and CSF Nf-L.